Electronic Supplementary Information for

Three-dimensional interpenetrating mesoporous carbon confining SnO_2 particles for superior sodiation/desodiation properties

Jagabandhu Patra [a], Purna Chandra Rath [b], Cheng-Hsein Yang [a], Diganta Saikia [b], Hsien-Ming Kao [b*], Jeng-Kuei Chang [a,c,d,*]

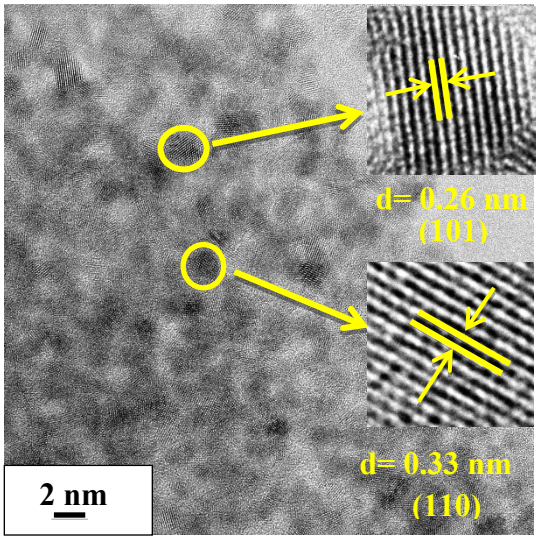

Figure S1. High-resolution TEM image of SnO_2/CMK-8 sample.

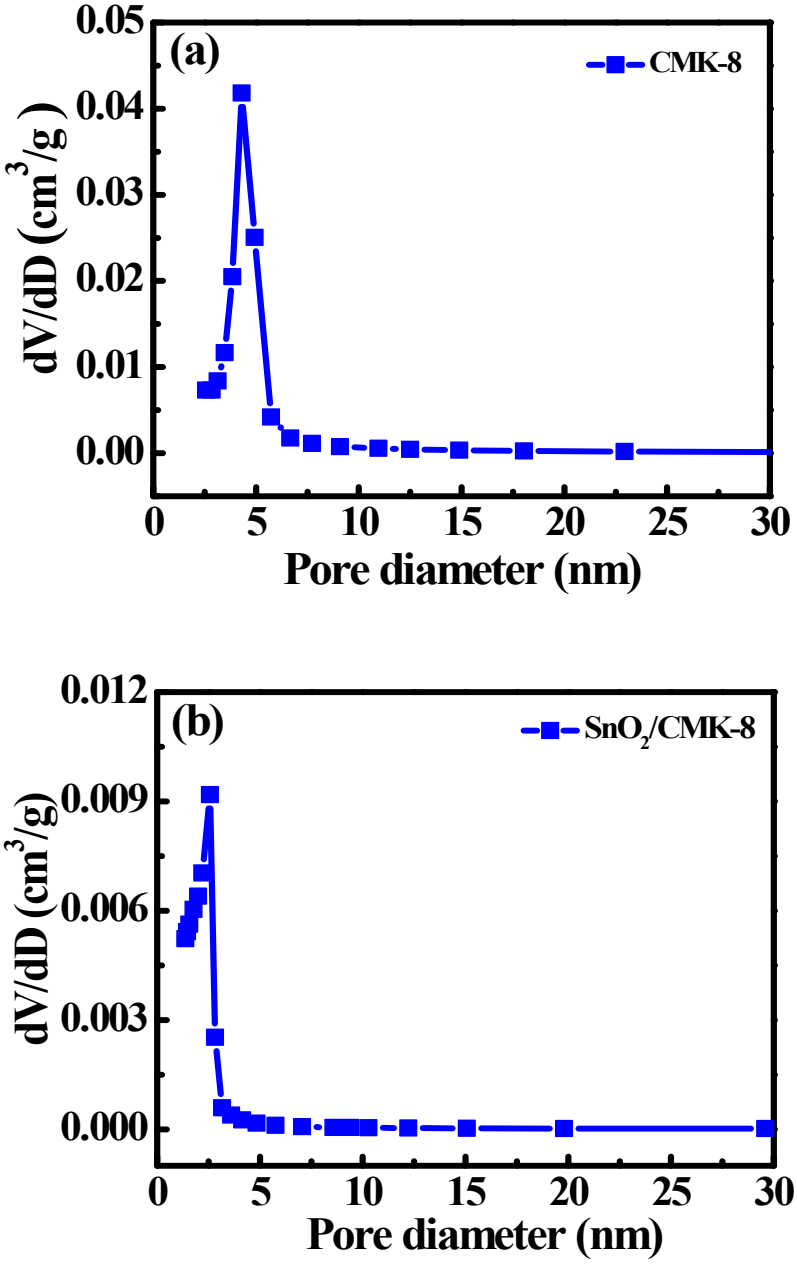

Figure S2. Pore size distribution data of (a) CMK and (b) SnO_2/CMK-8.

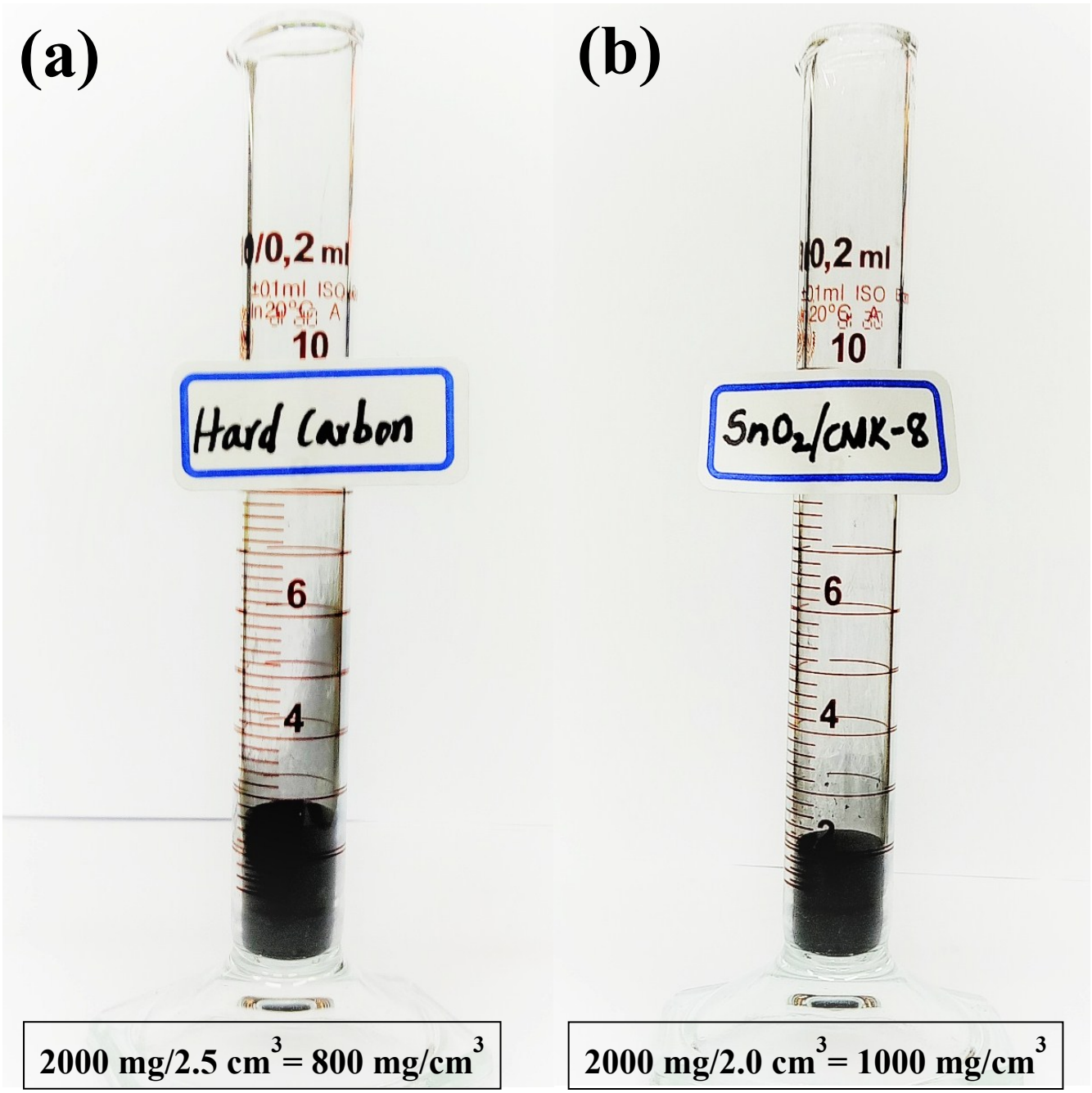

Figure S3. Tap densities of (a) commercial hard carbon and (b) SnO_2/CMK-8.

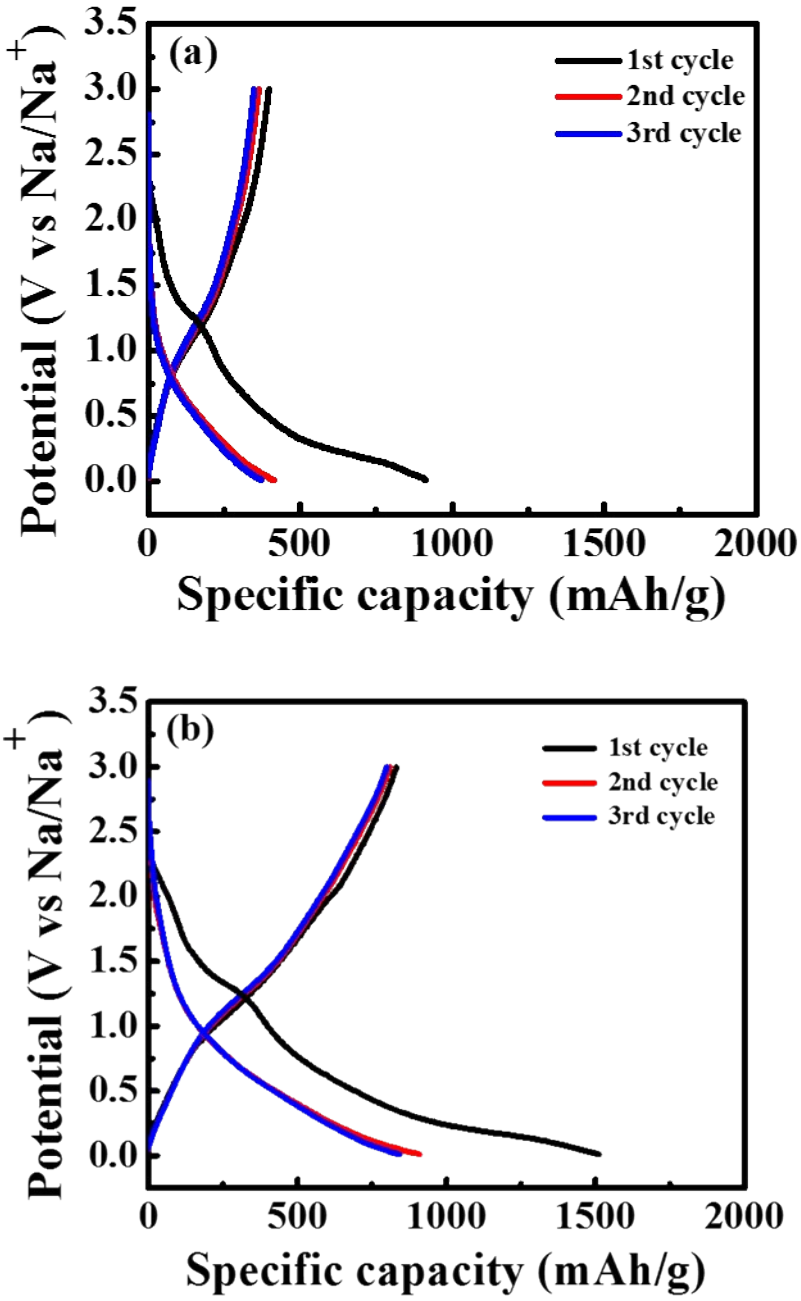

Figure S4. Initial three charge–discharge cycles of (a) plain SnO_2 and (b) SnO_2/CMK-8 electrodes measured at rate of 20 mA g^{-1}.

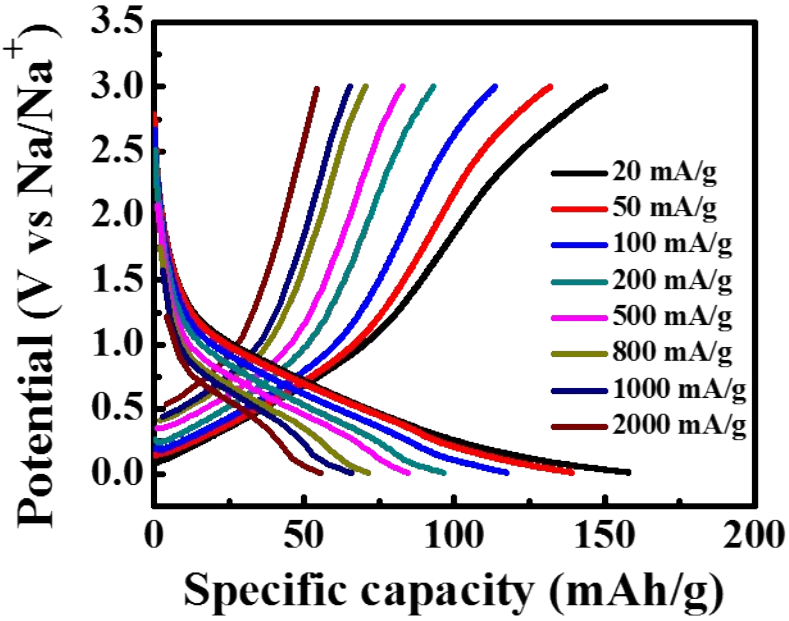

Figure S5. Charge–discharge curves of plain CMK-8 electrode recorded at various rates.

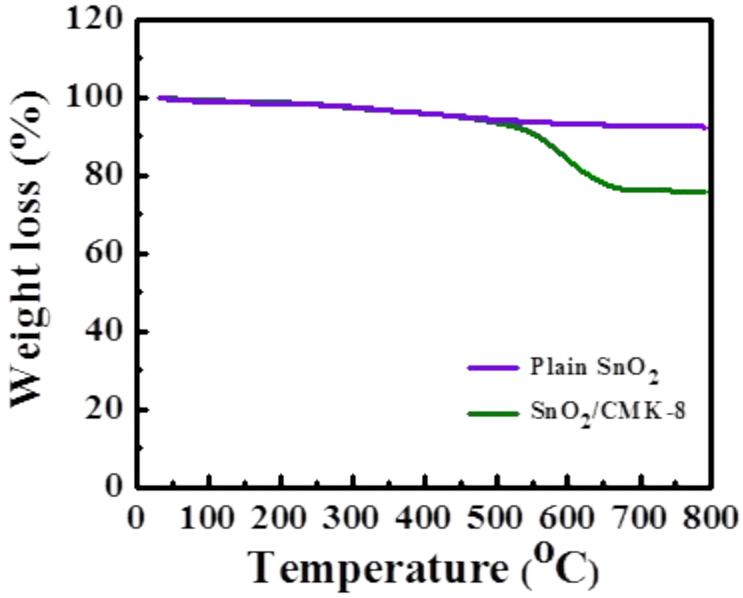

Figure S6. TGA data of plain SnO_2 and SnO_2/CMK-8 samples recorded under air with heating rate of 5 °C min^{-1}.

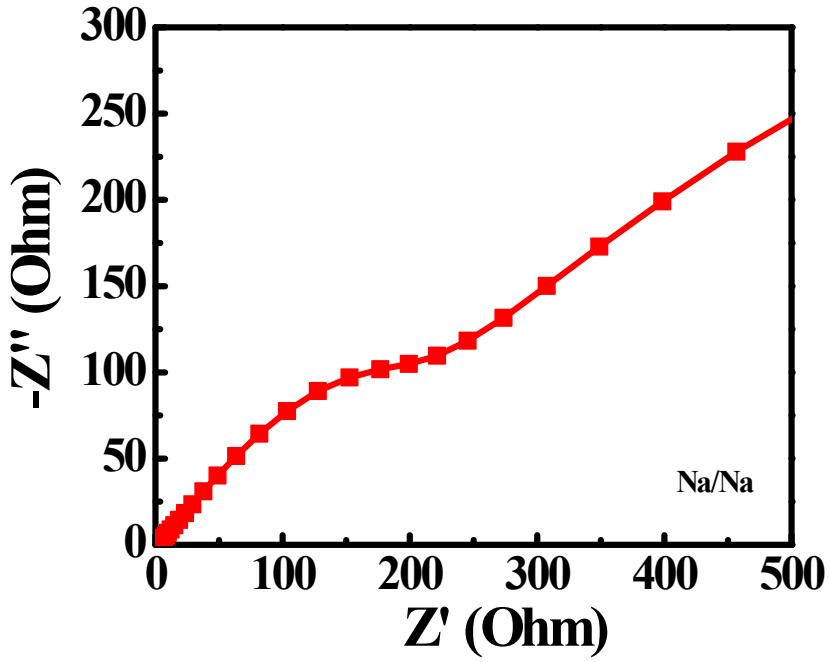

Figure S7. EIS data of Na/Na symmetric cell. The fitted R_{ct} value is ~400Ω, which is the sum of charge transfer resistances at both Na electrodes. This indicates that resistance at each Na electrode is ~200 Ω.

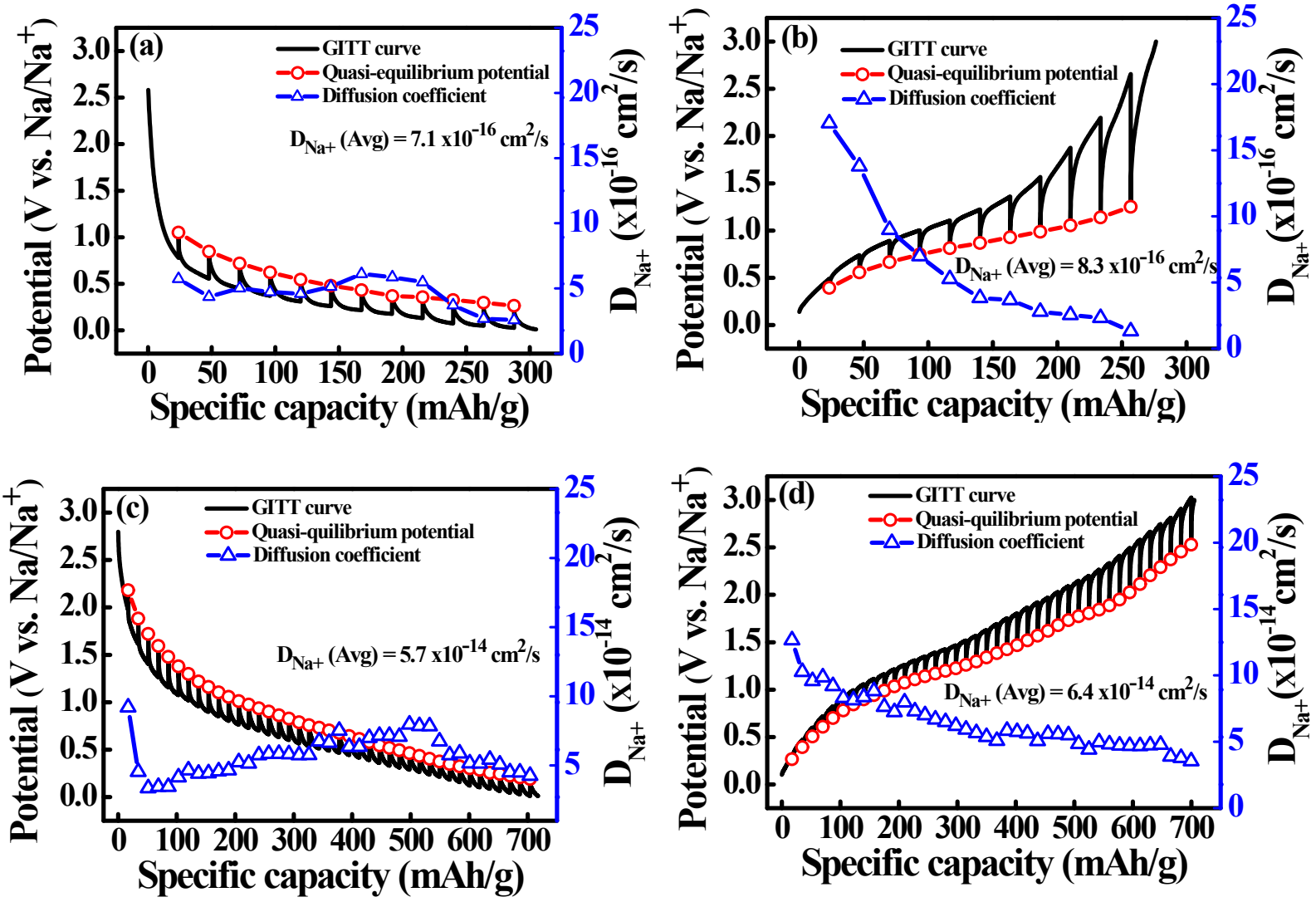

Figure S8. Quasi-equilibrium potentials and Na diffusion coefficients measured by GITT for (a, b) plain SnO_2 and (c, d) SnO_2/CMK-8 electrodes. Data were recorded with a series of current pulses of 50 mA g^{-1} for 20 min and 3 h relaxation at each interval.

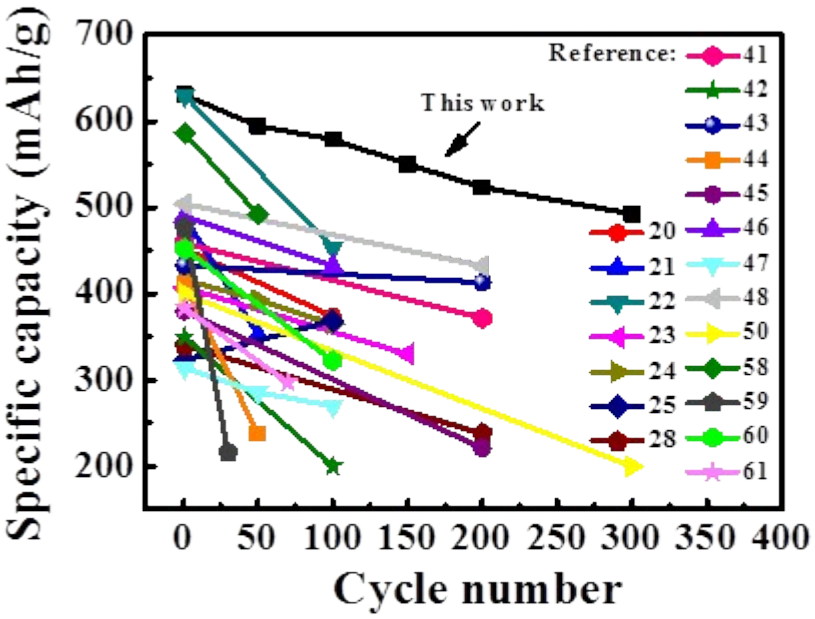

Figure S9. Cyclic stability comparison of proposed SnO_2/CMK-8 electrode and state-of-the-art SnO_2-based NIB anodes reported in the literature.

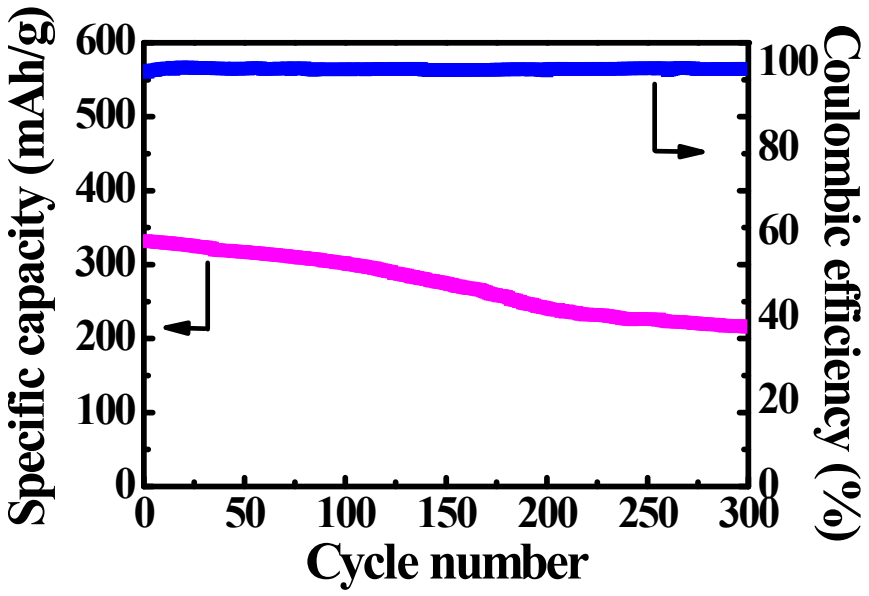

Figure S10. Cycling stability data of SnO_2/CMK-8 electrode measured at charge–discharge rate of 2000 mA g^{-1}.

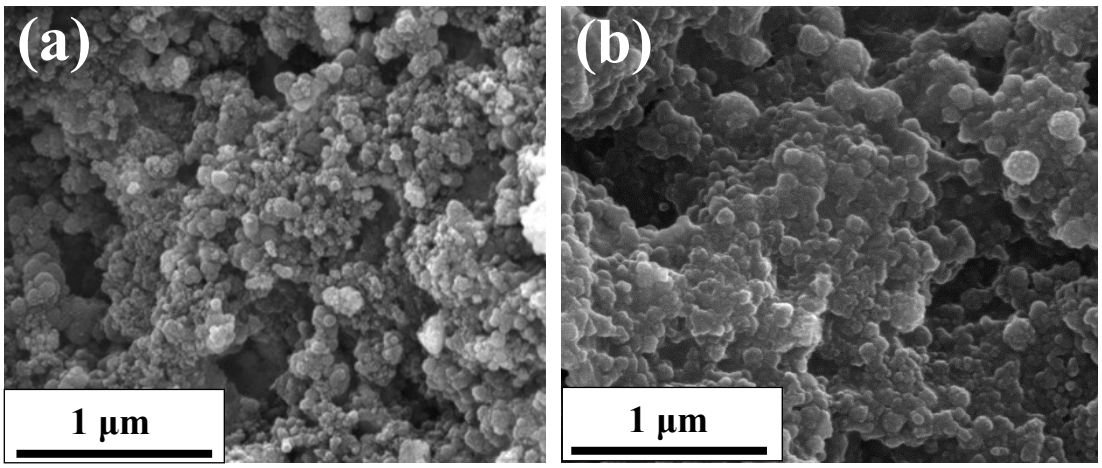

Figure S11. SEM images of SnO_2/CMK-8 electrode (a) before and (b) after 300 charge–discharge cycles.